Role of Solvent–Oxygen Ion Pairs in Photooxidation of CdSe Nanocrystal Quantum Dots

Virginia W. Manner,[†,§] Alexey Y. Koposov,[†] Paul Szymanski,[†,⊥] Victor I. Klimov,[†,‡,*] and Milan Sykora[†,*]

[†]Chemistry Division and [‡]Center for Advanced Solar Photophysics, Los Alamos National Laboratory, Los Alamos, New Mexico 87545, United States. [§]Present address: Explosives Applications and Special Projects, Los Alamos National Laboratory, Los Alamos, NM 87545. [⊥]Present address: Laser Dynamics Laboratory, School of Chemistry and Biochemistry, Georgia Institute of Technology, Atlanta, GA 30332.

ABSTRACT Understanding the mechanisms for photodegradation of nanocrystal quantum dots is an important step toward their application in real-world technologies. A usual assumption is that photochemical modifications in nanocrystals, such as their photooxidation, are triggered by absorption of a photon in the dot itself. Here, we demonstrate that, contrary to this commonly accepted picture, nanocrystal oxidation can be initiated by photoexcitation of solvent–oxygen ion pairs that relax to produce singlet oxygen, which then reacts with the nanocrystals. We make this conclusion on the basis of photolysis studies of solutions of CdSe nanocrystals. Our measurements indicate a sharp spectral onset for photooxidation, which depends on solvent identity and is 4.8 eV for hexane and 3.4 eV for toluene. Importantly, the photooxidation onset correlates with the position of a new optical absorption feature, which develops in a neat solvent upon its exposure to oxygen. This provides direct evidence that nanocrystal photooxidation is mediated by excitation of solvent–oxygen pairs and suggests that the stability of the nanocrystals is defined by not only the properties of their surfaces (as has been commonly believed) but also the properties of their environment, that is, of the surrounding solvent or matrix.

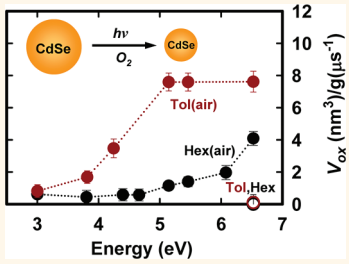

KEYWORDS: nanocrystals · quantum dots · oxidation · photooxidation · degradation · photochemistry

Nanocrystal (NC) quantum dots have the potential to enable a new generation of optoelectronic devices that can be processed from solutions using inexpensive scalable techniques such as ink-jet printing.[1,2] An important step toward a broad practical utilization of the NCs is the development of understanding the sources of their chemical and photochemical instabilities. Recently, we have shown that, in the case of PbSe NCs, processes such as thermally induced oxidation[3] and photoionization[4] can cause dramatic changes in optical properties of the NCs and their surface composition. While cadmium chalcogenides are generally more stable than their lead-based counterparts, they were also shown to be susceptible to thermal oxidation under specific conditions.[5,6] Upon photoexcitation, CdSe NCs were shown to undergo photocatalytic decomposition of the organic passivating layer,[7] photoionization,[8−10] or photooxidation[11−13] with the rates of these processes depending on the type of NC surface passivation and specific experimental conditions. While important insights were gained in previous studies, the understanding of the factors that affect the efficiency and rate of chemical and photochemical degradation of NCs is still limited.

In the present work, we use absorption spectroscopy to investigate the photochemical stability of tri-*n*-octylphosphine oxide (TOPO)-capped CdSe NCs in hexane and toluene during exposure to pulsed or steady-state radiation with various photon energies. Contrary to a common opinion that photodegradation of the NCs is initiated by absorption of a photon in the NC itself, we observe that in the case of irradiation with high-energy ultraviolet (UV) photons this process is dominated by photoexcitation of solvent–oxygen pairs. Specifically, we first establish a key role of oxygen in the observed photochemical reaction by comparing the effect of light on samples in inert atmosphere *versus* those exposed to oxygen. Then, we study the spectral dependence of photooxidation and detect a well-defined activation threshold. This threshold varies with solvent and is higher for hexane (~4.8 eV) than toluene (~3.4 eV). Interestingly, for both solvents, the onset for oxidation correlates with the spectral position of a new absorption feature, which develops in a neat solvent upon its exposure to oxygen. On the basis of these observations, we propose a mechanism for NC

* Address correspondence to sykoram@lanl.gov, klimov@lanl.gov.

Received for review November 28, 2011 and accepted March 1, 2012.

Published online March 01, 2012
10.1021/nn2046289

photooxidation, which involves interactions of the NCs with molecules of excited-state, singlet oxygen ($^1\Delta_g O_2$). These highly reactive species are formed as a transient product during relaxation of solvent−oxygen ion pairs excited by UV radiation.

RESULTS AND DISCUSSION

The NCs used in this work were synthesized and purified under argon atmosphere by modified literature methods.[14] For the studies under argon-equilibrated, air-free (AF) conditions, the fabricated samples were dissolved in hexane or toluene and transferred into cuvettes in an argon-filled glovebox. The solutions remained in sealed, air-tight cuvettes during measurements. For the studies of air-exposed (AE) samples, the cuvette with the NCs was open to atmosphere at ambient conditions to allow for equilibration with air. The equilibration of solutions with oxygen or water vapor was achieved by bubbling oxygen- or water-saturated argon gas through the NC solution in an air-tight cuvette for ~10 min. Longer exposure to gases did not lead to additional changes in optical properties of the NC solutions. In the monochromatic photolysis experiments, the excitation light was derived from a regeneratively amplified Ti:sapphire laser producing ~150 fs, 1.55 eV pulses at 250 kHz repetition rate. Harmonic generation in nonlinear optical crystals was used to produce light with 3.1, 4.6, or 6.2 eV photon energies. In the white-light photolysis experiments, a 75 W xenon (Xe) lamp (excitation power at the sample ~100 mW cm^{-2}) was used as a light source, and the width of the excitation spectrum was selected with appropriate low-pass cutoff filters. See methods section and Supporting Information (SI) for more details.

Figure 1 shows the observed changes in absorption spectra of the NCs in AF and AE hexane solutions upon pulsed excitation at energies of 3.1 eV (400 nm) or 6.2 eV (200 nm). The data in panel "a" show changes in the absorption spectra of the AE sample induced by continuous pulsed excitation at 6.2 eV. The exposure of the NCs to 6.2 eV radiation leads to a high-energy shift of the 1s peak, its broadening, and the overall reduction of the sample absorptivity. All of these changes are indicative of photodegradation of the NCs, which leads to the reduction of the mean CdSe core radius and the increase in size polydispersity.[3] No changes in the absorption spectra were detected in either AF or AE solutions with the 3.1 eV excitation and also in the AF solution under 6.2 eV excitation. These results are summarized in panel "b", which shows the shifts of the 1s peak in the AF and AE samples during the photolysis under 3.1 and 6.2 eV excitation. We note that no significant NC degradation was observed upon excitation of hexane solutions of NCs with 4.6 eV radiation, indicating that the activation threshold for the degradation processes in hexane is located between 4.6 and 6.2 eV.

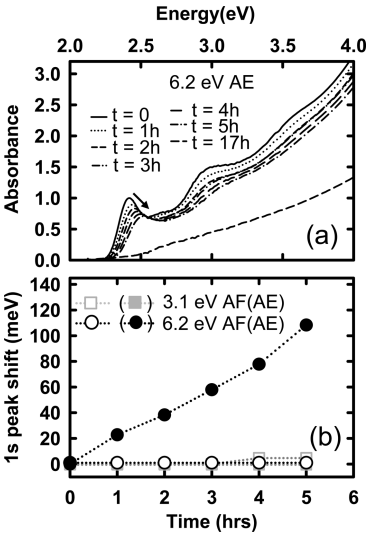

Figure 1. (a) Changes in the absorption spectra of the air-equilibrated solution of CdSe NCs (E_g = 2.41 eV) recorded during photolysis with 6.2 eV pulsed laser irradiation. Samples were continuously stirred during the irradiation. The arrow indicates the direction of the shift in the 1s peak as a result of photolysis. (b) Shift of the 1s peak maximum of the same NCs as in (a), but in argon-equilibrated (AF) and air-equilibrated (AE) hexane solution, recorded during the photolysis with 3.1 and 6.2 eV pulsed laser irradiation. The excitation was provided by frequency doubled (3.1 eV) and quadrupled (6.2 eV) pulses (~150 fs) of an amplified Ti: sapphire laser operating at the 250 kHz repetition rate. In all measurements, the pump fluence corresponded to $\langle N_{abs} \rangle$ of less than 0.01; $\langle N_{abs} \rangle$ is the average number of photons absorbed per pulse per NC.

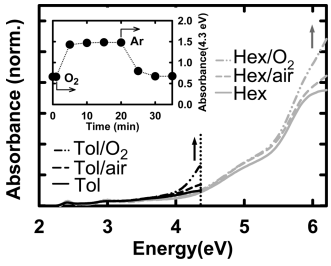

Figure 2. Absorption spectra of CdSe NCs in hexane and toluene in Ar-equilibrated solution, following exposure to air or O_2. The dotted lines indicate the solvent cutoff energy defined as the energy at which the solvent optical density is greater than 1. The inset shows the variation in absorbance of a toluene solution of the NCs at 4.3 eV following equilibration with O_2 and subsequent equilibration with Ar.

To further understand the effects of exposure of NC solutions to various components of air, we have carefully analyzed optical properties of the NC solutions following their equilibration with air-, oxygen-, and water-saturated argon gas. In Figure 2, the absorption spectra of the NCs in AF hexane and toluene are compared with the spectra of the same solutions following the equilibration with air or oxygen. Interestingly, exposure of the samples to either gas leads to the development of a new absorption feature at the energy which is close to the onset of solvent absorption.

The onset energies are ~4.3 eV in toluene and ~6 eV in hexane. The new absorption feature is more pronounced in the oxygen-equilibrated sample than in the sample equilibrated with air. The inset of Figure 2 shows that the effect of air/oxygen exposure on optical absorption can be reversed by equilibrating the solution with Ar. This indicates that the new absorption feature is due to a new electronic transition associated with the presence of oxygen in the solution. The transition could in principle be associated with interactions between the NC surfaces and dissolved oxygen. However, as discussed in greater detail below, the same new feature is observed in neat solvents under exposure to oxygen, indicating that it is the property of the solvents, not the NCs. The exposure of the solutions to the water-saturated Ar led to no significant changes in the absorption spectra of the NCs. The connection between our observations summarized in Figures 1 and 2 is discussed in more detail below.

The effect of high-energy radiation on absorption spectra of AE-exposed samples, shown in Figure 1, can be explained by photooxidation of the NC surface, which leads to progressive reduction of the average NC size and broadening of the size distribution. The fact that the effects of photooxidation are observed only at high excitation energies (>4.6 eV in hexane) suggests that there is an inherent energy barrier associated with this process. To determine the activation threshold for photooxidation, we performed photolysis of AF and AE NC solutions using filtered white light. In these experiments, the broad-band white light from a Xe lamp was transmitted through low-pass optical filters with varied cutoff energies (see methods and SI). The extent of NC photooxidation was measured in terms of the shift in the 1s absorption peak. The results of photolysis of NCs in AE hexane are shown in Figure 3a. As the filter cutoff energy is reduced from 6.53 to 6.05 eV (190 to 205 nm), then 5.15 eV (241 nm) and finally 3.00 eV (413 nm), the 1s spectral shift is also reduced from 72 to 29 meV and 14 and 5 meV, respectively; in wavelength, the spectral shift changes from 23 to 7 nm, then 4 nm, and finally 2 nm.

Figure 3b shows the photolysis results for hexane and toluene NC solutions presented in terms of the NC volume consumed during photooxidation (V_{ox}) for 60 min exposure to the filtered white light. These data were corrected for filter-to-filter variations in the total photon flux by normalizing V_{ox} by the excitation rate, g (see methods). The values of V_{ox} were obtained from the measurements of the 1s peak shift using the empirical relationship between the NC band gap energy and the NC radius.[15] While no appreciable effect of exposure to light on the 1s peak position is detected under AF conditions (open symbols), the AE solvents (solid symbols) exhibit clear signatures of oxidation: the blue shift of the 1s peak is indicative of the reduction of the NC volume. The oxidation rate increases sharply

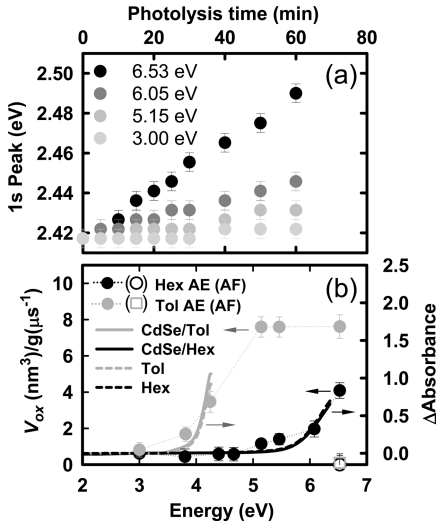

Figure 3. (a) Shifts of 1s peak maximum of the CdSe NCs recorded for the air-equilibrated hexane solution during the photolysis with filtered white light from a 75 W Xe lamp. The legend indicates the cutoff energies of the filters, defined as the energy above which less than 1% of incident light is transmitted. The concentration was adjusted so that the absorbance at the 1s peak was within 10% of 0.3. Samples were not stirred during the experiment. (b) Symbols show the reduction in the volume of the NCs calculated from the shift of the 1s peak following 60 min irradiation with filtered white light in argon- and air-equilibrated hexane and toluene. The horizontal axis is the filter cutoff energy, and the vertical axis shows the decrease in the mean NC volume corrected for variations in the total photon flux for different filters. The solid lines show the difference spectra generated by subtraction of the absorption spectrum of the argon-equilibrated solution of the NCs from the oxygen-equilibrated solution of the NCs. The dashed lines are the difference spectra generated in the same way for the neat solvents. For both solvents, the difference spectra are shown up to the solvent cutoff energy, where transmittance is <1%.

above a certain spectral energy, which we define as the activation threshold E_a. Interestingly, the thresholds are significantly different for hexane and toluene solutions and are ~4.8 and ~3.4 eV, respectively.[16] One possible explanation is that the higher solubility (concentration) of oxygen in one of the solvents contributes to reduction of the observed E_a. However, at room temperature, oxygen solubility is about a factor of two lower in toluene than in hexane (mole fractions: $x_{n\text{-hexane}}^{O_2} = 2.0 \times 10^{-3}$, $x_{\text{toluene}}^{O_2} = 9.2 \times 10^{-4}$),[17] which is inconsistent with the trend observed for the E_a values. Alternatively, the differences in the E_a values could be attributed to the differences in the surface properties of the NCs (*e.g.*, structure of the passivating layer) in the two solvents. While this may be a contributing factor, the analysis summarized in the following paragraphs indicates that the observed difference in E_a values is predominantly due to the difference in the properties of the solvent.

To elucidate the reasons for the difference in E_a values in hexane and toluene, in Figure 3b, we compare the photolysis results with the results of absorption

studies from Figure 2. The threshold of photooxidation (Figure 3b) matches very closely the onset of the new absorption features, which develop upon exposure of the NC solutions (or neat solvents) to air or oxygen (Figure 2). This match is apparent when we compare the photolysis results (symbols in Figure 3b) with the difference spectra generated from the data of Figure 2 by subtraction spectra of the AF and the oxygen-equilibrated NC solutions (solid lines in Figure 3b). In the same plot, we also show that the difference spectra of the neat solvents obtained in the same way (dashed lines in Figure 3b) closely overlap with the difference spectra of NC solutions. As was mentioned earlier, this indicates that the new absorption features observed in either solvent following air or oxygen exposure are associated with the solvent rather than the NCs. A close match between E_a and the onset of these oxygen-exposure-induced features further points toward an important role of new oxygen-related electronic transitions in the photooxidation of the NCs.

The distortion of the absorption spectra of organic molecules as a result of exposure to oxygen or air is a well-known phenomenon first reported in the 1950s[18,19] and studied extensively since then.[20−22] These studies showed that for most organic solvents the exposure to oxygen leads to a red shift of the onset of optical absorption with the shift magnitude directly related to the solvent ionization potential.[18−22] This new absorption feature was assigned to a transition from a weakly bound, ground state solvent−oxygen complex (Solv−O_2) to the contact charge-transfer pair (CCTP), typically represented as an excited state complex with a substantial solvent-radical-cation and oxygen-radical-anion characters, $Solv^{+\bullet}O_2^{-\bullet}$.[23] The CCTPs are short-lived species, decaying either directly or through an intermediate solvent triplet state to the ground state Solv−O_2, with typical lifetimes of less than 300 ps[24,25] (Scheme 1). A transient product formed during the CCTP relaxation is a singlet oxygen molecule, $^1\Delta_gO_2$, which in nonpolar organic solvents is produced with the quantum yield of >40%.[21,26] Due to restrictions associated with several selection rules, the $^1\Delta_gO_2$ relaxes slowly with lifetimes τ_Δ(hexane) = 31.4 μs and τ_Δ(toluene) = 28.5 μs.[27,28] Photochemical studies of many organic compounds have shown that both CCTPs and $^1\Delta_gO_2$ are highly reactive species which can effectively oxidize and oxygenate the solvent and/or dissolved substrates.[29−31]

Our results indicate that CCTPs play an important role in the process of NC oxidation studied here. We propose the following model to explain our observations. Above the activation threshold, the excitation of the contact Solv−O_2 complexes (Solv = hexane or toluene) leads to formation of CCTPs. The CCTPs relax rapidly, forming a population of $^1\Delta_gO_2$ molecules within the excitation volume. During their lifetime, the $^1\Delta_gO_2$ molecules diffuse, collide, and chemically

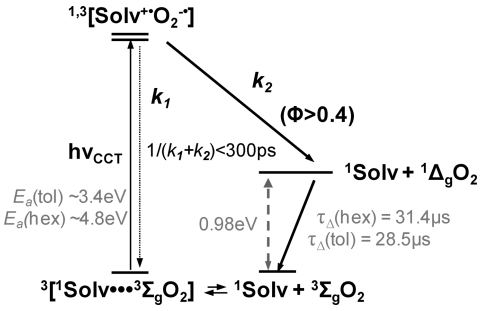

Scheme 1. Simplified diagram showing formation and relaxation of CCTP in hexane and toluene solutions.

react with the NCs. While the CCTPs could also, in principle, chemically react with the NCs, given the short lifetimes of the CCTPs, such interactions are unlikely, unless the CCTPs are formed directly at the NC surfaces.[32] The chemical activity of $^1\Delta_gO_2$ toward Cd chalcogenides was demonstrated in a recent study of degradation of CdTe NCs in aqueous solutions.[33] Specifically, it was shown that the $^1\Delta_gO_2$ molecules, formed *via* sensitized *NC-to-$^3\Sigma_gO_2$ energy transfer, effectively oxidize the CdTe NCs. In the case of CdSe NCs, the formation of $^1\Delta_gO_2$ mediated by energy transfer from the NCs is approximately 5% efficient.[28] The $^1\Delta_gO_2$ formed through this mechanism is likely responsible for the small spectral shifts observed below the activation threshold in our photolysis experiments. The larger spectral shifts, that is, more efficient photooxidation of the NCs, observed above the activation threshold, are attributed to a different mechanism where the formation of $^1\Delta_gO_2$ is mediated by photogenerated CCTPs. As mentioned earlier, in this process, $^1\Delta_gO_2$ is generated with >40% efficiency for every photon absorbed by Solv−O_2. With the absorption of the Solv−O_2 sharply increasing at high energies (Figures 2 and 3b), the concentration of $^1\Delta_gO_2$ in the excitation volume rapidly increases with increasing excitation energy up to the solvent cutoff energy, above which the incident photons cannot effectively penetrate through the solvent.

The efficiency of the photooxidation, η_{ox}(%), at a given excitation energy can be estimated from the magnitude of the observed spectral shifts and the measured incident photon flux. Here we define photooxidation efficiency as $\eta_{ox}(\%) = 100\%(N_{ox}/N_{abs})$, where N_{ox} is the number of oxidized NC atoms, estimated from the spectral shift, and N_{abs} is the total number of photons absorbed by the sample during the irradiation period (see methods). Using this definition, we calculate that for the hexane solution of the CdSe NCs with optical density 0.13 at 1s peak (conc. $\sim 1.3 \times 10^{-5}$ M),[15] excited with pulsed monochromatic light at 6.2 eV, η_{ox} is ~1%. This fairly low efficiency of the photooxidation process explains why significant spectral shifts in the absorption spectra of the air-exposed NCs, for excitation intensities used here, are observed only on the

time scales of minutes to hours. Since, according to the proposed mechanism, the photooxidation is a diffusion-controlled process, the η_{ox} is expected to vary with number of factors, such as oxygen solubility, concentration of NCs, as well as temperature and the solvent viscosity. Our studies indicate that η_{ox}, in fact, decreases with increasing NC concentration. We attribute this observation to the reduced efficiency of formation of CCTPs due to the screening of the incident radiation by the NCs.

The oxidation of CdSe NCs has been investigated by several groups.[5,6,12,13,34] Studies of air-exposed CdSe NC films have shown that both thermal oxidation and photooxidation of the NCs by ground state oxygen ($^3\Sigma_gO_2$) are observed under specific conditions.[5,6,12,13] In solutions, on the other hand, thermal oxidation of CdSe NCs by $^3\Sigma_gO_2$ was shown to be inefficient.[34] Our photolysis studies of air- or oxygen-equilibrated solutions, at excitation energies below the CCTP formation threshold, suggest that photooxidation of CdSe NCs by $^3\Sigma_gO_2$ is also likely inefficient.[35] Clear signatures of photooxidation are, however, observed under the conditions when $^1\Delta_gO_2$ is formed. This is consistent with the fact that the excess energy (~0.98 V)[36] stored transiently in the $^1\Delta_gO_2$ makes it a significantly better oxidant than $^3\Sigma_gO_2$. As a result, the oxidation of CdSe NCs by $^1\Delta_gO_2$ is thermodynamically more favorable by ~22.5 kcal/mol. Our results suggest that this excess driving force is necessary to overcome kinetic barriers to oxidation of CdSe NCs in solutions.

CONCLUSIONS

In conclusion, we have studied the photochemical stability of CdSe NCs in air-free and air-exposed hexane and toluene solutions. We have found that excitation with high-energy photons of air-exposed solutions leads to efficient photoinduced oxidation of the NCs. We show that, contrary to expectation, the photooxidation is not NC initiated, but rather a solvent-initiated process involving solvent−oxygen ion pairs and their relaxation transient product, singlet oxygen. We have determined the activation energies of this process in hexane and toluene solvents that are, respectively, ~4.8 and ~3.4 eV. These findings suggest that the properties of environment have significant impact on the stability of colloidal nanocrystals, and the improvement of their resistance to photooxidation may require the control of the properties of the surrounding solvent or matrix.

METHODS

Syntheses and Sample Preparation. Unless otherwise noted, all reagents were purchased from Aldrich and solvents from Fisher. For the preparation of the CdSe NCs, $CdMe_2$ was purchased from Strem Chemicals; TOPO (tech grade, 90%) and TOP (tech grade, 90%) were purchased from Aldrich (batch # 06820CH, 07596KJ, respectively); Se shot (99.999%) was purchased from Alfa Aesar; "extra dry" hexane, toluene, and methanol were purchased from ACROS Organics. These chemicals were used without any additional purification.

The CdSe NCs were synthesized under air-free conditions following the procedure described in our recent report.[14] The solutions of the NCs used in the physical measurements were prepared inside an argon-filled glovebox following the procedure described in the same report. In a typical experiment, a TOPO-growth solution of NCs (0.4 g) was washed once in hexane/MeOH (0.3 mL/2 mL) before the NCs were dissolved in hexane or benzonitrile. The NC solution was then diluted and transferred to a 1 mm or a 1 cm path length air-free cuvette equipped with Viton O-ring valves. Solutions to be air-equilibrated were brought outside the glovebox and thoroughly mixed with air before being placed in the cuvettes fitted with Teflon stoppers.

Monochromatic Photolysis Measurements. For the monochromatic photolysis measurements, the air-free or air-exposed NC solutions were transferred to 1 mm cuvettes. The equilibration of solutions with oxygen was achieved by bubbling oxygen gas through the air-free NC solution in 1 mm air-tight cuvette for ~10 min. The optical density of all solutions was 0.1−0.2. In an experiment, the excitation was provided by a regeneratively amplified Ti:sapphire laser system (Coherent RegA) operating at 250 kHz. The pulse width was ~150 fs. Harmonic generation in BBO crystals was used to produce pump pulses with energies 3.1 or 6.2 eV, with residual 1.55 eV laser fundamental removed by band-pass filters or prisms. The pump fluence was adjusted to correspond to <0.01 photons absorbed/nanocrystal at the front face of the cuvette. The samples were continuously stirred during the irradiation. The absorption spectra were collected using an Agilent 8453 UV−visible spectrophotometer in absorbance mode.

The photooxidation efficiency, η_{ox}, defined as $\eta_{ox}(\%) = 100 \times N_{ox}/N_{abs}$ (where N_{ox} = number of oxidized atoms and N_{abs} = number of photons absorbed by the sample), was determined in following way. The number of photons adsorbed by the sample was calculated using expression: $N_{abs} = n_g$-(per second) $\times f_A \times t$(s), where N_{abs} is the number of photons absorbed by the sample over the irradiation time period, f_A is fraction of light absorbed by the sample at the excitation energy, defined as $f_A = 1-10^{-A}$, and t(s) is the irradiation time in seconds. The term n_g represents the number of incident photons per second calculated as $n = j_i \times \lambda/hc$, where j_i is the incident irradiation energy in Joules per second, λ is the wavelength of the excitation irradiation, h is Planck constant, and c is the speed of light. The average number of oxidized atoms per NC was estimated from the shift in the 1s peak absorption observed during the photolysis. First, the change in the average volume of the NCs was estimated from the shift in the 1s peak position using an empirical relationship between the position of 1s peak and NC radius.[15] The change in volume was converted to the number of oxidized atoms using relationship:[37] $\langle n_{ox}\rangle = 2 \times \rho(g/cm^3) \times N_a(mol^{-1}) \times \Delta V(cm^3)/M(g/mol)$, where $\langle n_{ox}\rangle$ is the number of oxidized atoms, ρ is CdSe density taken as 5.674 g/cm^3, N_a is Avogadro's constant, ΔV is the change in volume, and M is the molar mass of the CdSe unit. The total number of oxidized atoms, N_{ox}, was calculated as $N_{ox} = N \times \langle n_{ox}\rangle$, where N is the total number of NCs in the sample calculated as $N = c \times N_a \times V$, where c is the sample concentration and V is its volume. In the calculation of the η_{ox}, we assumed that the Cd and Se atoms were oxidized with equal efficiency.

Broad-Band Photolysis Measurements. In the broad-band photolysis measurements, a standard quartz cuvette (1 cm path length) containing 2.3 mL of air-free or air-exposed NC solution was placed in a holder approximately 15 cm from the irradiation source. The concentration of the NCs in solution was adjusted so that the absorbance at the 1s peak was within 10% of 0.3. The irradiation source was a 75 W xenon lamp (Newport). The

circular beam of light incident on the sample had a diameter of ~1 cm, or the beam was defocused to uniformly irradiate the entire sample. The samples were not stirred during the experiment. The light intensity was measured before the data collection using an optical power meter (in an independent measurement, we have previously verified that the variation in the source light intensity was less than 2% over the course of 1 h). In a typical experiment, the absorption spectrum of the sample was taken before the irradiation and then every 5 min for the first half hour and every 10 min thereafter. The absorption spectra were collected using an Agilent 8453 UV−visible spectrophotometer in absorbance mode.

Adjustment of the Excitation Spectral Range. To adjust the spectral range of the light used in the photolysis, the white light from the Xe lamp was filtered using custom optical filters prepared by filling 1 cm quartz cuvettes with various solvents (or their combination). In the control "unfiltered" experiments, an empty quartz cuvette was substituted for the filters. Figure S1 in SI shows UV−visible spectra of the prepared filters. The cutoff wavelength of the filter was defined as the wavelength at which the absorbance was greater than or equal to 2. During the experiment, the sides of the filter were masked so that light could only pass directly through the filter. In the case of 413, 502, and 551 nm cutoff wavelengths, we used commercial long-pass filters. The power of the filtered light at the sample position was measured before each measurement and, regardless of the filter used, generally fell in the range of 210 ± 20 mW (Figure S2).

Determination of the Corrected Oxidized Volume, $V_{ox}(cm^3)/g(\mu s^{-1})$. In Figure 3b, we express the efficiency of the photooxidation in terms of NC oxidized volume $V_{ox}(cm^3)$ corrected for different NC exciton generation rates, $g(\mu s^{-1})$, under different irradiation conditions. In determining the corrected oxidized volume, first the V_{ox} was estimated from observed spectral shifts as described above. The exciton generation rate was calculated as $g(\mu s^{-1}) = A\int_\lambda N_p(\lambda)\sigma(\lambda)T_f(\lambda)$, where A is the cross-section area of the excitation beam at the sample, $N_p(\lambda)$ is number of incident photons, $\sigma(\lambda)$ is the absorption cross section of the NCs, and $T_f(\lambda)$ is the transmittance of the filter in percent. The $N_p(\lambda)$ for the Xe lamp was determined by an independent measurement using a calibrated Si photodetector. The $\sigma(400)$ was calculated using previously reported empirical relationship.[38] The σ values for other wavelengths were obtained by scaling the experimentally measured absorption spectrum of the NCs to match calculated $\sigma(400)$. The $T_f(\lambda)$ values for each of the filters were determined experimentally.

Conflict of Interest: The authors declare no competing financial interest.

Acknowledgment. V.W.M., A.Y.K., P. S., and M.S. acknowledge support of the Los Alamos Directed Research and Development Funds. V.I.K. is supported by the Center for Advanced Solar Photophysics, an Energy Frontier Research Center funded by the U.S. Department of Energy, Office of Science, Office of Basic Energy Sciences. We thank Dr. David Thorn for helpful discussions.

Supporting Information Available: Additional details of broad-band photolysis studies and CCTP spectra of solvents commonly used in studies of NCs. This material is available free of charge *via* the Internet at http://pubs.acs.org.

REFERENCES AND NOTES

1. Talapin, D. V.; Lee, J. S.; Kovalenko, M. V.; Shevchenko, E. V. Prospects of Colloidal Nanocrystals for Electronic and Optoelectronic Applications. *Chem. Rev.* **2010**, *110*, 389–458.
2. Klimov, V. I. *Semiconductor and Metal Nanocrystals. Synthesis and Electronic and Optical Properties*; Marcel Dekker: New York, 2004.
3. Sykora, M.; Koposov, A. Y.; McGuire, J. A.; Schulze, R. K.; Tretiak, O.; Pietryga, J. M.; Klimov, V. I. Effect of Air Exposure on Surface Properties, Electronic Structure, and Carrier Relaxation in PbSe Nanocrystals. *ACS Nano* **2010**, *4*, 2021–2034.
4. McGuire, J. A.; Sykora, M.; Robel, I.; Padilha, L. A.; Joo, J.; Pietryga, J. M.; Klimov, V. I. Spectroscopic Signatures of Photocharging Due to Hot-Carrier Transfer in Solutions of Semiconductor Nanocrystals under Low-Intensity Ultraviolet Excitation. *ACS Nano* **2010**, *4*, 6087–6097.
5. Katari, J. E. B.; Colvin, V. L.; Alivisatos, A. P. X-ray Photoelectron-Spectroscopy of CdSe Nanocrystals with Applications to Studies of the Nanocrystal Surface. *J. Phys. Chem.* **1994**, *98*, 4109–4117.
6. Dabbousi, B. O.; Rodriguez-Viejo, J.; Mikulec, F. V.; Heine, J. R.; Mattoussi, H.; Ober, R.; Jensen, K. F.; Bawendi, M. G. (CdSe)ZnS Core−Shell Quantum Dots: Synthesis and Characterization of a Size Series of Highly Luminescent Nanocrystallites. *J. Phys. Chem. B* **1997**, *101*, 9463–9475.
7. Aldana, J.; Wang, Y. A.; Peng, X. G. Photochemical Instability of CdSe Nanocrystals Coated by Hydrophilic Thiols. *J. Am. Chem. Soc.* **2001**, *123*, 8844–8850.
8. Krauss, T. D.; Brus, L. E. Charge, Polarizability, and Photoionization of Single Semiconductor Nanocrystals. *Phys. Rev. Lett.* **1999**, *83*, 4840–4843.
9. Uematsu, T.; Maenosono, S.; Yamaguchi, Y. Photoinduced Fluorescence Enhancement in Mono- and Multilayer Films of CdSe/ZnS Quantum Dots: Dependence on Intensity and Wavelength of Excitation Light. *J. Phys. Chem. B* **2005**, *109*, 8613–8618.
10. Li, S.; Steigerwald, M. L.; Brus, L. E. Surface States in the Photoionization of High-Quality CdSe Core/Shell Nanocrystals. *ACS Nano* **2009**, *3*, 1267–1273.
11. Jasieniak, J.; Mulvaney, P. From Cd-Rich to Se-Rich: The Manipulation of CdSe Nanocrystal Surface Stoichiometry. *J. Am. Chem. Soc.* **2007**, *129*, 2841–2848.
12. van Sark, W. G. J. H. M.; Frederix, P. L. T. M.; Bol, A. A.; Gerritsen, H. C.; Meijerink, A. Blueing, Bleaching, and Blinking of Single CdSe/ZnS Quantum Dots. *ChemPhysChem* **2002**, *3*, 871–879.
13. Nazzal, A. Y.; Wang, X. Y.; Qu, L. H.; Yu, W.; Wang, Y. J.; Peng, X. G.; Xiao, M. Environmental Effects on Photoluminescence of Highly Luminescent CdSe and CdSe/ZnS Core/Shell Nanocrystals in Polymer Thin Films. *J. Phys. Chem. B* **2004**, *108*, 5507–5515.
14. Koposov, A. Y.; Szymanski, P.; Cardolaccia, T.; Meyer, T. J.; Klimov, V. I.; Sykora, M. Electronic Properties and Structure of Assemblies of CdSe Nanocrystal Quantum Dots and Ru-Polypyridine Complexes Probed by Steady State and Time-Resolved Photoluminescence. *Adv. Funct. Mater.* **2011**, *21*, 3159–3168.
15. Yu, W. W.; Qu, L. H.; Guo, W. Z.; Peng, X. G. Experimental Determination of the Extinction Coefficient of CdTe, CdSe, and CdS Nanocrystals. *Chem. Mater.* **2003**, *15*, 2854–2860.
16. We note that photolysis of AF hexane and toluene solutions of NCs with a small amount of AF water leads to gradual precipitation of NCs but no apparent spectral shifts.
17. Battino, R.; Rettich, T. R.; Tominaga, T. The Solubility of Oxygen and Ozone in Liquids. *J. Phys. Chem. Ref. Data* **1983**, *12*, 163–178.
18. Evans, D. F. Molecular Association of Oxygen and Aromatic Substances. *J. Chem. Soc.* **1953**, 345–347.
19. Munck, A. U.; Scott, J. F. Ultra-Violet Absorption of Oxygen in Organic Solvents. *Nature* **1956**, *177*, 587.
20. Gooding, E. A.; Serak, K. R.; Ogilby, P. R. Ground-State Benzene Oxygen Complex. *J. Phys. Chem.* **1991**, *95*, 7868–7871.
21. Scurlock, R. D.; Ogilby, P. R. Singlet Molecular Oxygen ($^1\Delta_gO_2$) Formation upon Irradiation of an Oxygen ($^3\Sigma_gO_2$)-Organic Molecule Charge-Transfer Absorption Band. *J. Phys. Chem.* **1989**, *93*, 5493–5500.
22. Tamres, M.; Strong, R. L. In *Molecular Association*; Foster, R., Ed.; Academic Press: London, 1979; Vol. 2, pp 331−456.
23. Tsubomura, H.; Mulliken, R. S. Molecular Complexes and Their Spectra 0.12. Ultraviolet Absorption Spectra Caused by the Interaction of Oxygen with Organic Molecules. *J. Am. Chem. Soc.* **1960**, *82*, 5966–5974.
24. Logunov, S. L.; Rodgers, M. A. J. Subnanosecond Dynamics of a Napthalene-Oxygen Exciplex. *J. Phys. Chem.* **1992**, *96*, 2913–2914.
25. Logunov, S. L.; Rodgers, M. A. J. Laser Flash-Photolysis Studies of the Contact Complex between Molecular-Oxygen and 1-Methylnaphtalene. *J. Phys. Chem.* **1993**, *97*, 5643–5648.

26. Scurlock, R. D.; Ogilby, P. R. Spectroscopic Evidence for the Formation of Singlet Molecular-Oxygen ($^1\Delta_gO_2$) upon Irradianation of a Solvent Oxygen ($^3\Sigma_gO_2$) Cooperative Absorption-Band. *J. Am. Chem. Soc.* **1988**, *110*, 640–641.
27. Rodgers, M. A. J. Solvent-Induced Deactivation of Singlet Oxygen: Additivity Relationships in Non-Aromatic Solvents. *J. Am. Chem. Soc.* **1983**, *105*, 6201–6205.
28. Samia, A. C. S.; Chen, X.; Burda, C. Semiconductor Quantum Dots for Photodynamic Therapy. *J. Am. Chem. Soc.* **2003**, *125*, 15736–15737.
29. McKeown, E.; Waters, W. A. Oxidation of Organic Compounds by Singlet Oxygen. *J. Chem. Soc. B* **1966**, 1040–1050.
30. Onodera, K.; Furusawa, G.; Kojima, M.; Tsuchiya, M.; Aihara, S.; Akaba, R.; Sakuragi, H.; Tokumaru, K. Mechanistic Considerations of Photoreaction of Organic Compounds *via* Excitation of Contact Charge Transfer Complexes with Oxygen. *Tetrahedron* **1985**, *41*, 2215–2220.
31. Komatsu, T.; Tsuchiya, M.; Furusawa, G.; Kuriyama, Y.; Sakuragi, H.; Nakanishi, F.; Tokumaru, K. Attempts at Direct Detection of Reactive Species in Selective Excitation of the Contact Charge Transfer Pairs of Hexamethylbenzene and Oxygen. *Bull. Chem. Soc. Jpn.* **1995**, *68*, 277–281.
32. Assuming the same diffusion coefficient, $D \sim 1 \times 10^{-6}$ cm^2/s for CCTPs and $^1\Delta_gO_2$, we can estimate that the diffusion length is ~0.2 and ~56 nm for the CCTPs and $^1\Delta_gO_2$, respectively.
33. Zhang, Y.; He, J.; Wang, P.-N.; Chen, J.-Y.; Lu, Z.-J.; Lu, D.-R.; Guo, J.; Wang, C.-C.; Yang, W.-L. Time-Dependent Photoluminescence Blue Shift of the Quantum Dots in Living Cells: Effect of Oxidation by Singlet Oxygen. *J. Am. Chem. Soc.* **2006**, *128*, 13396–13401.
34. Myung, N.; Bae, Y.; Bard, A. J. Enhancement of the Photoluminescence of CdSe Nanocrystals Dispersed in $CHCl_3$ by Oxygen Passivation of Surface States. *Nano Lett.* **2003**, *3*, 747–749.
35. We note that both the reaction mechanism and the efficiency of photoxidation are likely to be affected by the NC surface composition and passivation. See for example: Jasieniak, J.; Mulvaney, P. From Cd-Rich to Se-Rich—The Manipulation of CdSe Nanocrystal Surface Stoichiometry. *J. Am. Chem. Soc.* **2007**, *129*, 2841–2848.
36. Schweitzer, C.; Schmidt, R. Physical Mechanisms of Generation and Deactivation of Singlet Oxygen. *Chem. Rev.* **2003**, *103*, 1685–1757.
37. Kuno, M.; Lee, J. K.; Dabbousi, B. O.; Mikulec, F. V.; Bawendi, M. G. The Band Edge Luminescence of Surface Modified CdSe Nanocrystallites: Probing the Luminescing State. *J. Chem. Phys.* **1997**, *106*, 9869–82.
38. Klimov, V. I. Optical Nonlinearities and Ultrafast Carrier Dynamics in Semiconductor Nanocrystals. *J. Phys. Chem. B* **2000**, *104*, 6112–6123.